Interaction of the conserved oligomeric Golgi complex with t-SNARE Syntaxin5a/Sed5 enhances intra-Golgi SNARE complex stability

Anna Shestakova, Elena Suvorova, Oleksandra Pavliv, Galimat Khaidakova, and Vladimir Lupashin

Department of Physiology and Biophysics, College of Medicine, University of Arkansas for Medical Sciences, Little Rock, AR 72205

Tethering factors mediate initial interaction of transport vesicles with target membranes. Soluble *N*-ethylmaleimide–sensitive fusion protein attachment protein receptors (SNAREs) enable consequent docking and membrane fusion. We demonstrate that the vesicle tether conserved oligomeric Golgi (COG) complex colocalizes and coimmunoprecipitates with intra-Golgi SNARE molecules. In yeast cells, the COG complex preferentially interacts with the SNARE complexes containing yeast Golgi target (t)-SNARE Sed5p. In mammalian cells, hCog4p and hCog6p interact with Syntaxin5a, the mammalian homologue of Sed5p. Moreover, fluorescence resonance energy transfer reveals an in vivo interaction between Syntaxin5a and the COG complex. Knockdown of the mammalian COG complex decreases Golgi SNARE mobility, produces an accumulation of free Syntaxin5, and decreases the steady-state levels of the intra-Golgi SNARE complex. Finally, overexpression of the hCog4p N-terminal Syntaxin5a-binding domain destabilizes intra-Golgi SNARE complexes, disrupting the Golgi. These data suggest that the COG complex orchestrates vesicular trafficking similarly in yeast and mammalian cells by binding to the t-SNARE Syntaxin5a/Sed5p and enhancing the stability of intra-Golgi SNARE complexes.

Introduction

In eukaryotes, membrane trafficking between organelles is mediated by transport carriers (vesicles and larger pleomorphic structures), which bud from donor membranes and then fuse to acceptor ones (Bonifacino and Glick, 2004). Vesicle targeting and fusion depends on the consequent action of the three protein families. The first is the coiled coil and oligomeric vesicle tethering factors, so called because they tether incoming transport intermediates to the acceptor membrane (for review see Sztul and Lupashin, 2006). The second is the Rab family of small GTPases (Pfeffer, 2001), which regulates vesicle tethering and docking. The third are SNAREs, which mediate fusion of the vesicle (v-SNARE) with the acceptor membrane (t-SNARE; Ungar and Hughson, 2003).

Correspondence to Vladimir Lupashin: vvlupashin@uams.edu

A. Shestakova's present address is Dept. of Biology, University of Utah, Salt Lake City, UT 84112.

E. Suvorova's present address is Dept. of Microbiology, Montana State University, Bozeman, Montana 59717.

Abbreviations used in this paper: AD, activation domain; BD, binding domain; COG, conserved oligomeric Golgi; FRET, fluorescence resonance energy transfer; GalNAcT2, *N*-acetylgalactosaminyltransferase-2; GARP, Golgi-associated retrograde protein; HOPS, homotypic fusion and vacuole protein sorting; IF, immunofluorescence; IP, immunoprecipitation; KD, knockdown; WB, western blotting.

The online version of this paper contains supplemental material.

Oligomeric vesicle tethering factors are evolutionarily conserved and comprise a structurally diverse group of peripheral membrane protein complexes that orchestrate close-range membrane-to-membrane interactions before SNARE complex assembly (Oka and Krieger, 2005). One subfamily includes the transport particles I and II and the homotypic fusion and vacuole protein sorting (HOPS) complexes that possess catalytic GDP–GTP exchange activity toward specific Rab proteins (Jones et al., 2000; Wang et al., 2000; Wurmser et al., 2000). Another subfamily of quatrefoil (a structure with four lobes) tethering factors, which includes conserved oligomeric Golgi (COG) complex, Golgi-associated retrograde protein (GARP), and exocyst complex (Whyte and Munro, 2001), does not show any particular catalytic activity toward components of the transport machinery but is known to interact with the activated form of organelle-specific Rab proteins (Guo et al., 1999; Siniossoglou and Pelham, 2001; Suvorova et al., 2002). These Rab–tether interactions may work to correctly position the tethering molecules on both donor and acceptor membranes. SNARE proteins act downstream of Rab proteins and, together with tethering factors, are believed to confer positional information ensuring high-fidelity vesicle fusion (Shorter et al., 2002).

Several oligomeric tethering complexes colocalize and directly interact with SNARE molecules (Price et al., 2000;

The Journal of Cell Biology, Vol. 179, No. 6, December 17, 2007 1179–1192
http://www.jcb.org/cgi/doi/10.1083/jcb.200705145

Suvorova et al., 2002; Fridmann-Sirkis et al., 2006), but the mechanism of this tether–SNARE interaction is not well understood. For example, the HOPS complex stably associates with v- and t-SNARE complexes on vacuoles before and after fusion (Stroupe et al., 2006). In this case, Vps33p, a subunit of the HOPS complex, directly binds to the t-SNARE Vam3 (Rieder and Emr, 1997). Sec6p, a subunit of the exocyst complex, binds in vitro to the plasma membrane t-SNARE Sec9p where it modulates the interaction between Sec9p and Sso1p (Sivaram et al., 2005). Vps51p, a subunit of the trans-Golgi–localized GARP complex, specifically binds to the conserved N-terminal domain of the t-SNARE Tlg1p. However, Vps51–Tlg1 interaction is not essential for GARP-mediated endosome trans-Golgi network trafficking (Fridmann-Sirkis et al., 2006).

The COG complex is a peripheral membrane heterooligomer found in yeast and mammalian cells. It consists of eight subunits named Cog 1–8 (Ungar et al., 2002). Based on yeast and mammalian genetic and biochemical studies (Whyte and Munro, 2001; Fotso et al., 2005; Oka et al., 2005; Ungar et al., 2005) and on electron microscopy (Ungar et al., 2002), the eight subunits of the COG complex were grouped into two subcomplexes: Cog 1–4 (Lobe A) and Cog 5–8 (Lobe B). The COG complex is involved in retrograde membrane trafficking of Golgi resident proteins, and thus mutations in the subunits of the COG complex severely alter localization and function of the Golgi glycosylation machinery (Kingsley et al., 1986; Whyte and Munro, 2001; Suvorova et al., 2002; Wu et al., 2004; Foulquier et al., 2006; Kubota et al., 2006; Shestakova et al., 2006).

Numerous genetic interactions have been detected between the COG complex and SNARE proteins (VanRheenen et al., 1998, 1999; Kim et al., 1999; Ram et al., 2002). We recently showed that the yeast COG complex coimmunoprecipitates with the Golgi t- and v-SNAREs Sed5p, Gos1p, Ykt6p, and Sec22p (Suvorova et al., 2002) and that the mammalian COG complex coimmunoprecipitates with GS28 the mammalian homologue of Gos1p (Zolov and Lupashin, 2005). Our data also indicate that the localization and stability of Golgi SNAREs are altered in cells expressing a defective COG complex (Oka et al., 2004; Fotso et al., 2005; Zolov and Lupashin, 2005; Shestakova et al., 2006). These findings led us to hypothesize that the COG complex regulates the formation and/or stability of the intra-Golgi SNARE complex.

Our results show that in yeast and mammalian cells the COG complex colocalizes and coimmunoprecipitates with intra-Golgi t- and v-SNARE molecules. We demonstrate that the COG–SNARE interaction is direct, bidirectional, and specific. Yeast COG complex specifically interacts in vitro with the SNARE domain of the Golgi t-SNARE Sed5p and preferentially binds to the quaternary Sed5p-containing SNARE complexes. We also show that the mammalian hCog4p subunit directly binds to Syntaxin5a, the mammalian homologue of Sed5p. In addition, fluorescence resonance energy transfer (FRET) experiments reveal a direct, spatially constricted in vivo interaction between Syntaxin5a and the COG complex. We show that defects in the mammalian COG complex function lead to a significant decrease in Golgi SNARE mobility, an accumulation of uncomplexed Syntaxin5, and a decrease in the steady-state level of intra-Golgi SNARE complexes. Collectively, these data suggest that the COG complex enhances stability of intra-Golgi SNARE complexes.

Results

Yeast COG complex interacts with the Sed5p SNARE domain and the Sed5p-containing SNARE complexes

Previous work from our lab and others (VanRheenen et al., 1998, 1999; Ram et al., 2002; Suvorova et al., 2002; Fotso et al., 2005) indicates that in yeast cells the COG complex interacts genetically and physically with a subset of Golgi SNARE molecules, for instance, Sed5p, Ykt6p, Gos1p, and Sec22p. The strongest in vitro interaction was observed with the Golgi t-SNARE Sed5p (Suvorova et al., 2002). Immunofluorescence (IF) microscopy shows colocalization of Sed5p and yCog3p in yeast cells (Fig. S1, available at http://www.jcb.org/cgi/content/full/jcb.200705145/DC1).

The yeast Sed5 protein (340 aa) can be dissected into the transmembrane domain (aa 324–340) and three evolutionarily conserved domains (Fig. 1 A): Sed5H1 (aa 1–78), Sed5H2 (aa 99–186), and Sed5H3 or SNARE domain (aa 208–324; Kosodo et al., 1998). In yeast cells, Sed5p physically interacts with the COPII component Sec24p (Peng et al., 2000), ER–Golgi GTPase Ypt1 (Lupashin and Waters, 1997), Sly1p (Søgaard et al., 1994), and at least seven different ER–Golgi and intra-Golgi SNARE proteins (Søgaard et al., 1994; Lupashin et al., 1997; von Mollard et al., 1997; Tsui et al., 2001). Previous experiments demonstrate that the Sed5H1 domain is essential for the protein's interaction with Sly1p (Kosodo et al., 1998; Bracher and Weissenhorn, 2002). Sed5H3 (SNARE domain) is essential for interaction with cognate SNAREs (Sacher et al., 1997) and Sec17p, an accessory protein involved in the disassembly of the SNARE complex (Kosodo et al., 1998). Because Sed5p interacts with proteins involved in membrane traffic (SNAREs and SNARE-associated proteins), we hypothesized that Sed5p might directly interact with the COG complex.

We set up an in vitro binding assay to study binding of the yeast COG complex to the different domains of Sed5p. Fig. 1 B indicates that the yeast COG complex binds efficiently to the full-length cytosolic portion of Sed5p and Sed5H3 (Fig. 1 B) and fourfold less efficiently to the Sed5H1 and Sed5H2 domains (Fig. 1 B, H1, H2, and H1 + 2). This specificity is confirmed by the absence of the COG subunits in the GST pulldown of the plasma membrane SNARE protein Sso1p (Fig. 1 B). Finally, a titration experiment shows that the yeast COG complex has similar affinity for Sed5p and the Sed5p SNARE domain (Fig. 1, C and D). Thus, the yeast COG complex preferentially binds to the SNARE domain of Sed5p.

Next, we examined the temporal and spatial interaction between Sed5p and the COG complex. We tested if the Sed5p–COG interaction is influenced by the formation of the SNARE complex. Sed5p alone and two different SNARE complexes containing Sed5p were bound to glutathione-Sepharose beads and tested for their ability to bind to the purified yeast COG complex (Fig. 2 A). Because bacterially expressed Ykt6p shows

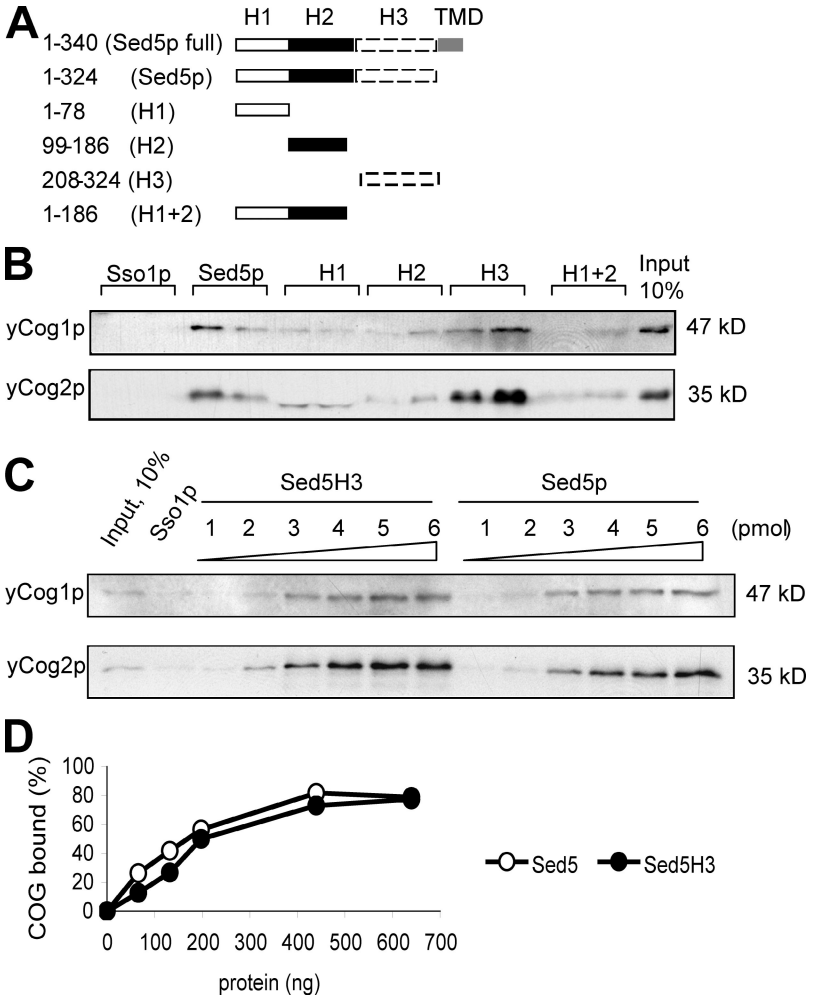

Figure 1. **Yeast COG complex interacts with the SNARE domain of Sed5p.** (A) Schematic representation of Sed5p domains. H3, SNARE domain; TMD, transmembrane domain. (B) In vitro binding assay of the cytosolic portion of Sed5p, Sed5H1, Sed5H2, Sed5H1 + 2, or Sed5H3 to the purified yeast COG complex. 10 µl glutathione-Sepharose beads slurry with prebound GST-tagged Sed5 proteins (5 pmol of each) were incubated for 4 h on ice with the purified yeast COG complex (TAP-yCog2p, 0.2 µg of total protein). Eluates were analyzed by immunoblotting with yeast anti-yCog1 and 2 antibodies. GST-Sso1p was used as a control for nonspecific binding. (C) Yeast COG complex has a similar affinity to Sed5p and Sed5p SNARE domain. Serial dilutions of glutathione-Sepharose beads with prebound GST-tagged proteins were prepared and the amount of GST proteins is indicated (picomoles). Protein-free glutathione-Sepharose beads were used to normalize the total volume of beads up to 10 µl. In vitro binding assay was performed as described in B. Western blots were scanned and protein recovery was calculated with ImageJ software. The results were plotted in a graph (D).

low efficiency of incorporation into Sed5p-containing SNARE complex, Ykt6p is substituted with Sec22p. Ykt6p and Sec22p are partially interchangeable in both in vivo and in vitro assays (Tsui et al., 2001; Liu and Barlowe, 2002). We show yeast COG complex to bind efficiently to both intra-Golgi [Sed5 + Sft1p + Sec22p + Gos1p] and ER–Golgi [Sed5p + Bet1p + Sec22p + Bos1p] SNARE complexes in vitro in a concentration-dependent manner (Fig. 2 A). Surprisingly, yeast COG complex binds to isolated Sed5p less efficiently than to the quaternary SNARE complexes with incorporated Sed5p (Fig. 2 A). The COG complex does not efficiently interact with single Golgi SNAREs (Fig. 2 B) with either binary [Gos1p + Sed5p] or ternary [Gos1p + Sed5p + Sec22p] complexes (not depicted). Thus, the COG complex preferentially binds to the complete quaternary SNARE bundle over the isolated SNAREs.

Mammalian COG complex is associated with the Golgi SNAREs

To test if the COG–SNARE association is evolutionarily conserved, we performed coimmunoprecipitation (co-IP) and colocalization studies of the mammalian COG complex and intra-Golgi SNAREs in HeLa cells. IP of the mammalian COG complex using affinity-purified α-hCog3p antibody from the detergent-solubilized purified rat liver Golgi membranes (Fig. 3 A) reveals that both rat Cog3p (Lobe A subunit) and rat Cog8p (Lobe B subunit) are efficiently coimmunoprecipitated (Fig. 3 A). Importantly, we show that up to 4% of Syntaxin5a, the mammalian Sed5p homologue, and its SNARE partner GS28 is coimmunoprecipitated with rat Cog3p (Fig. 3 A). Bet1p, an ER–Golgi SNARE partner of Syntaxin5a, is not coimmunoprecipitated with rat Cog3p, which reveals a specificity of the COG–SNARE interaction (Fig. 3 A). Intriguingly, 10% of Golgi matrix protein GM130 and 4% of vesicle-tethering factor p115 are also coimmunoprecipitated with rat Cog3p (Fig. 3 A), indicating cross talk between coiled coil and oligomeric tethers (Sohda et al., 2007). Abundant protein disulfide isomerase is not detected in the IP (Fig. 3 A, PDI). In agreement with our co-IP results, in live HeLa cells, YFP-Cog3p colocalizes with DsRed-Syntaxin5a in a perinuclear Golgi region (Fig. 3 B, arrows) and both proteins are mostly excluded from the ER.

We previously demonstrated that Sed5p is isolated with the yeast COG complex. Noticeably, yCog4p (TFI3) was the most efficient binding partner of Sed5p (Fig. 7 in Suvorova et al., 2002). We used yeast two-hybrid assay to identify the subunit of the mammalian COG complex that directly interacts with intra-Golgi SNARE molecules (Fig. 4 A). Full-length subunits of the mammalian COG complex were fused to the C-terminus of Gal4 binding domain (BD; Ungar et al., 2005).

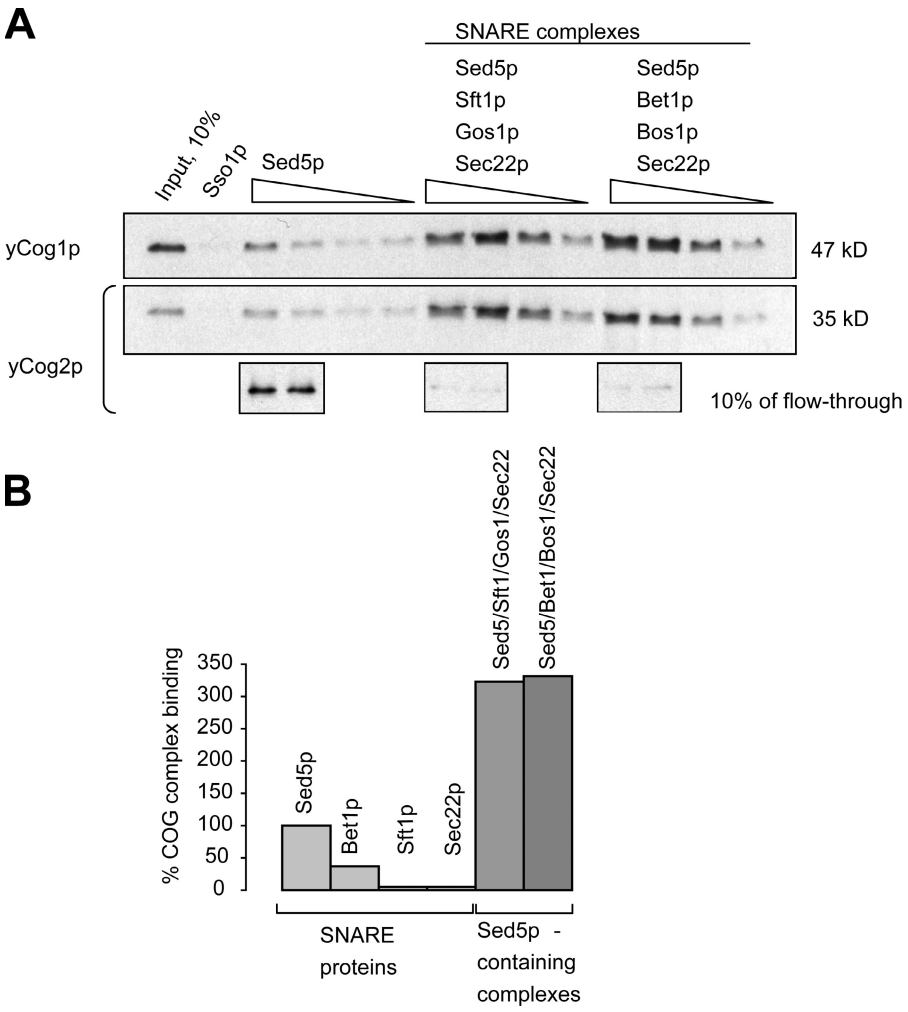

Figure 2. **Yeast COG complex preferentially binds to the preformed SNARE complexes in vitro.** (A) 5 pmol each of [His-Sed5 + GST-Bet1 + His-Bos1 + His-Sec22] or [His-Sed5 + GST-Sft1 + His-Gos1 + His-Sec22] was incubated overnight on ice. Preformed SNARE complexes were purified on TALON resin, bound to 10 µl glutathione-Sepharose beads, and incubated on ice for 4 h with 40 ng of the purified yeast COG complex. GST-tagged proteins were eluted. Eluates were analyzed by immunoblotting with yeast anti-yCog1p and anti-yCog2p antibodies. (B) Bands corresponding to the yCog1p and yCog2p from three independent binding experiments with individual GST-tagged SNAREs and preformed SNARE complexes were quantified using ImageJ software and the result was plotted in a bar graph. Efficiency of the COG complex binding to 200 ng Sed5p was taken for 100%.

The cytoplasmic portion of the mammalian Golgi SNAREs Syntaxin5a, Syntaxin6, GS28, GS15, membrin, and Bet1p were fused to the Gal4 activation domain (AD). Except Syntaxin5a, none of the tested Golgi SNAREs shows an interaction with the subunits of the COG complex. Moreover, BD-hCog1p, 2p, 5p, and 7p did not interact with any SNARE molecules. BD-hCog3p, 4p, and 8p showed autoactivation when coexpressed with empty AD vector, and thus ability to grow on –HIS but not –ADE plates (unpublished data). Importantly, Syntaxin5a is the only SNARE molecule that interacts with the subunits of the COG complex. hCog4p and 6p show strong and weak interactions, respectively, with Syntaxin5a as demonstrated by the diploid growth on –ADE and –HIS plates (Fig. 4 A). This hCog4p–Syntaxin5a interaction is as strong as previously described intra-COG complex interactions between hCog4p and 2p (Ungar et al., 2005). Conversely, yeast two-hybrid assay revealed interaction between BD-Syntaxin5a and AD-hCog4, 5, 6, and 8 proteins (Fig. S2 A, available at http://www.jcb.org/cgi/content/full/jcb.200705145/DC1). Subsequent yeast two-hybrid tests showed preferential binding of hCog4p to the H3 domain (aa 180–281) of Syntaxin5a (Fig. S2 B). Thus, both direct and reverse yeast two-hybrid data indicate that hCog4p and 6p are direct binding partners of Syntaxin5a. The putative interaction between Syntaxin5a and two additional subunits of Lobe B of the COG complex (hCog5p and 8p) may be either an artifact of yeast two-hybrid assay or, alternatively, may indicate an additional multifaceted COG–SNARE interaction that will be investigated elsewhere. Further truncation analysis of hCog4p reveals that its N-terminal fragment (1–222 aa) is sufficient for the interaction with Syntaxin5a (Fig. 4 A).

To further confirm the yeast two-hybrid interaction between Syntaxin5a and the hCog4p and hCog6p subunits, both GFP-Syntaxin5a and myc-tagged hCog4p and 6p were coexpressed in HeLa cells (Fig. 4, B and C). hCog4p and 6p myc-tagged fusions are coimmunoprecipitated with GFP-Syntaxin5a but not with GFP alone (Fig. 4 B, compare GFP [lanes 1 and 2] and GFP-Syntaxin5a [lanes 3–6]). Importantly, the N-terminal 1–222-aa fragment of hCog4p is efficiently coimmunoprecipitated with GFP-Syntaxin5a. More than 10% of 1–222 hCog4p can be copurified with GFP-Syntaxin5a (Fig. 4 B, lane 5′). A shorter 150-aa hCog4p polypeptide is coimmunoprecipitated with GFP-Syntaxin5a less efficiently (Fig. 4 B, lane 6'). A reciprocal IP with anti-myc antibody (Fig. 4 C) confirms specificity of the COG–Syntaxin5a interaction. The highest copurification of GFP-Syntaxin5a is observed in cells that express 1–222 hCog4p (Fig. 4 C, lane 5′). Interestingly, hCog3p is copurified with the full-length but not with 1–222 hCog4p (unpublished data), indicating direct protein–protein interaction between Syntaxin5a and 1–222 hCog4p. Thus, the full-length hCog4p

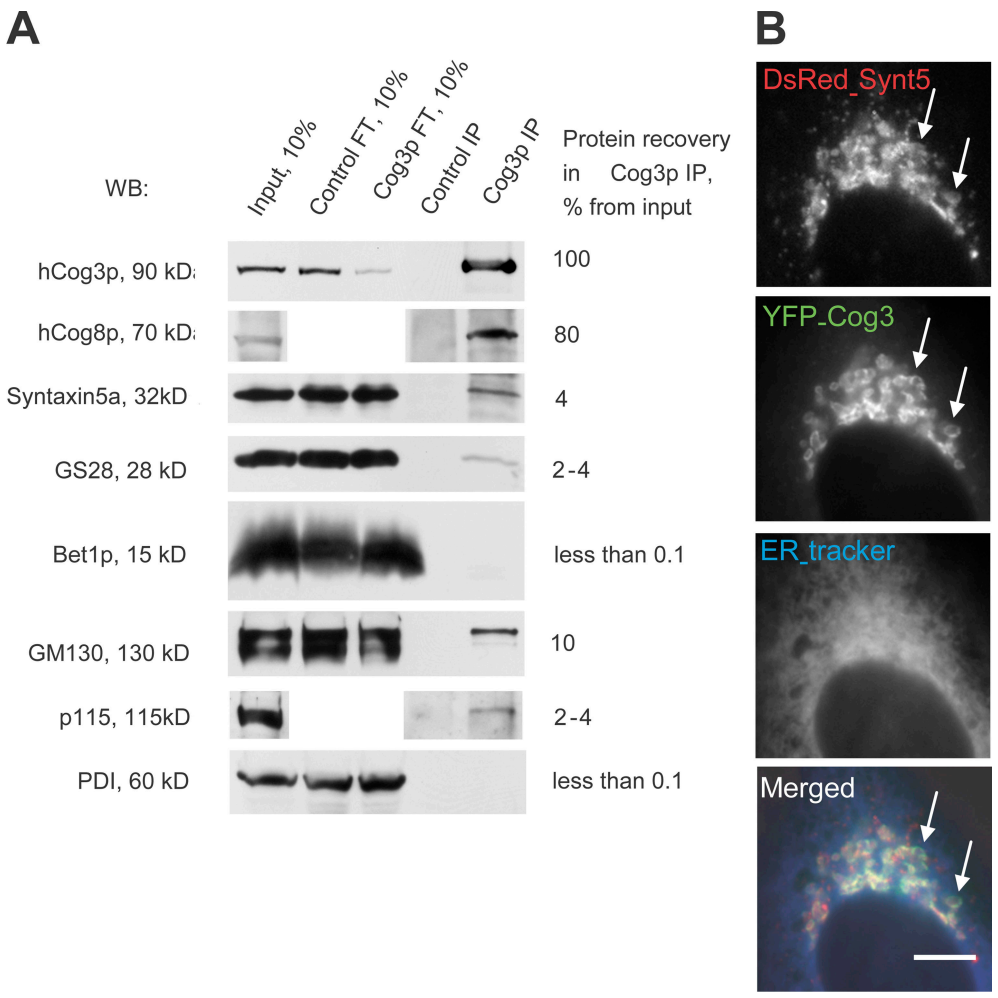

Figure 3. **Mammalian COG complex interacts and colocalizes with intra-Golgi SNAREs.** (A) Protein complexes were immunoprecipitated with preimmune (Control IP) or affinity-purified anti-hCog3p antibody (α-hCog3 IP) from rat liver Golgi CHAPS extract. 10% of Golgi extract and flow through (FT) fractions, as well as 100% IP, was analyzed by immunoblotting with indicated antibodies. Western blots were quantified by ImageJ software. The percentage of the recovery of each protein in α-hCog3p IP (relative to the recovery of rat Cog3p) is shown. (B) DsRed-Syntaxin5a and YFP-hCog3p colocalize on Golgi membrane. HeLa cells stably expressing YFP-hCog3p were transfected with plasmid expressing DsRed-Syntaxin5a. 24 h after transfection, the ER was labeled with an ER tracker and the fluorescent proteins in live cells were visualized using a microscope. Arrows indicate colocalization of the proteins on the Golgi membranes. Bar, 10 μm.

and hCog6p, as well as the first 222 aa of hCog4p are reciprocally coimmunoprecipitated with Syntaxin5a.

To further substantiate the interaction of Syntaxin5a with the COG complex in vivo, we used FRET. Our preliminary experiments suggest that the GFP tag interferes with incorporation of hCog4p into the endogenous COG complex (unpublished data). Previously, we generated a cell line stably expressing YFP-hCog3p at an adequate protein level and YFP-hCog3p was incorporated into the endogenous COG complex (Suvorova et al., 2001). Because hCog3p and 4p belong to Lobe A of the COG complex (Ungar et al., 2005), we followed the energy transfer between YFP-hCog3p and CFP-Syntaxin5a. Indeed, CFP-Syntaxin5a colocalizes with YFP-hCog3p in the Golgi region (Fig. 5 A, arrowhead) and the level of expression is similar to that of the endogenous (Fig. 5 E). We detect a 15% increase in CFP-Syntaxin5a fluorescence after photobleaching YFP-hCog3p, indicating efficient FRET between the two molecules (Fig. 5 D). Analysis of the CFP fluorescence before (Fig. 5 A) and after (Fig. 5 B) YFP photobleaching reveals that Syntaxin5a and the COG complex efficiently interact only on the limited Golgi subdomains (Fig. 5 C, arrows, FRET signal). It is thus tempting to suggest that these Golgi subdomains may be the trafficking hot spots, with a high concentration of Syntaxin5a primed for SNARE complex formation (Williams et al., 2004). Similar FRET signal is detected between CFP-hCog6p and YFP-hCog3p, whereas FRET is not detected between other Golgi-localized SNAREs, CFP-Syntaxin6 and YFP-hCog3p (Fig. S3, available at http://www/jcb.org/cgi/content/full/jcb.200705145/DC1). The increase of CFP-Syntaxin5a fluorescence after the YFP-hCog3 photobleach suggests that these proteins interact in vivo.

Defective COG complex decreases mobility of SNAREs and destabilizes the Golgi SNARE complex

We previously showed that COG3 siRNA knockdown (KD) results in a redistribution of GS15 into the vesicles that are dispersed throughout the cytoplasm (Zolov and Lupashin, 2005). COG7 siRNA KD affects the distribution of GS15 less dramatically

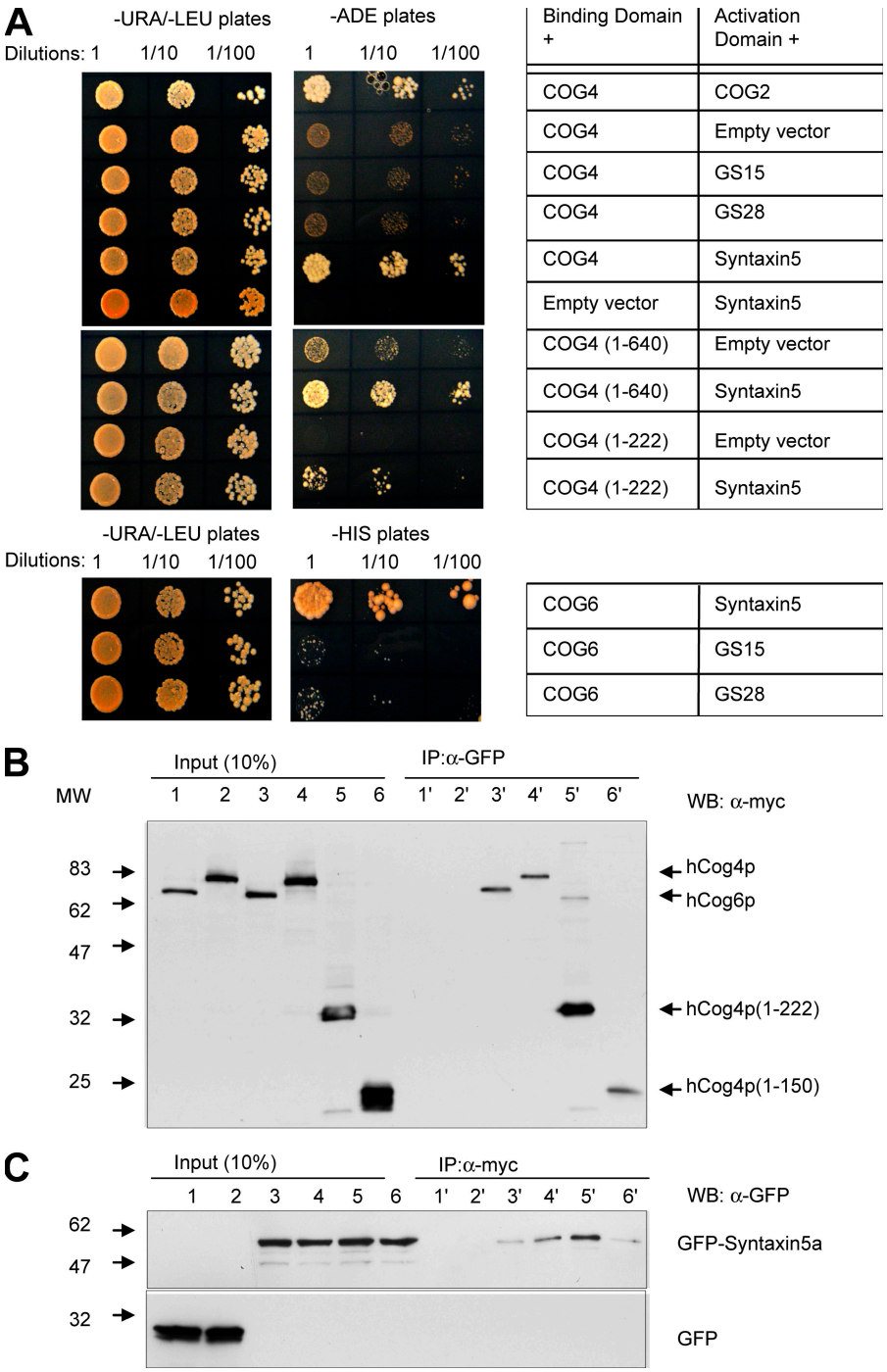

Figure 4. **Syntaxin5a interacts with hCog4p and hCog6p.** (A) Yeast two-hybrid assay. Yeast diploids coexpressing hCog1-8 GAL4 BD fusions and Golgi SNAREs GAL4 AD fusions were grown in liquid selective media to OD_{600} = 1.0. Serial dilutions (total 10 µl) of yeast cells were applied on agar plates lacking uracil and leucine (−URA/−LEU) for diploid growth, adenine (−ADE) for strong interaction, or histidine (−HIS) for weak interaction. Yeast diploids were scored for growth after 72 h at 30°C. (B and C) hCog4p and 6p coimmunoprecipitate with GFP-Syntaxin5a. HeLa cells were cotransfected with plasmids (1 and 1′, GFP/hCog6-myc; 2 and 2′, GFP/hCog4-myc; 3 and 3′, GFP-Syntaxin5a/hCog6-myc; 4 and 4′, GFP-Syntaxin5a/hCog4-myc; 5 and 5′, GFP-Syntaxin5a/hCog4(1–222)-myc; and 6 and 6′, GFP-Syntaxin5a/hCog4(1–150)-myc). 24 h after transfection, cells were lysed in PBS with 1% Triton X-100 and proteins from the S20-soluble fraction were immunoprecipitated with anti-GFP (B) or anti-myc (C) antibodies. 10% of S20 (Input) as well as entire immunoprecipitate (eluate) were analyzed by Western blot using anti-myc (B) or -GFP (C) antibodies.

with a majority of GS15 localized to the perinuclear region (Shestakova et al., 2006). GFP-GS15 and GFP-Syntaxin5a localize to the perinuclear Golgi membranes in control cells (Fig. 6, B and E). As expected, COG7 KD results in a fragmentation of GFP-positive Golgi membranes (Fig. 6, C and F), suggesting a crucial role for the COG complex in maintaining Golgi integrity.

To estimate the relative mobility of the tagged SNARE molecules in both control and COG7 KD cells, we used FRAP. The bleaching of a small area (<10% of the Golgi surface) of the control cells results in a relatively fast recovery of a GFP-GS15 signal with $t_{1/2}$ of ∼100 s (Fig. 6 A, squares). At the same time, GFP-Syntaxin5a fluorescence recovers slower, with $t_{1/2}$ of ∼220 s (Fig. 6 D, diamonds). hCog7p depletion causes a significant delay in the recovery of both v- and t-SNARE molecules with $t_{1/2}$ of > 500 s (Fig. 6, A and D, circles), indicating restricted mobility of intra-Golgi SNAREs, GS15, and Syntaxin5a in COG7 KD cells. Decreased mobility of Golgi SNARE proteins may indicate either a block in the formation of SNARE complexes or their entrapment into stable frozen complexes.

In agreement with previously published results (Williams et al., 2004), a conformation-specific monoclonal antibody, 18C8, which binds only to free (uncomplexed) Syntaxin5 but

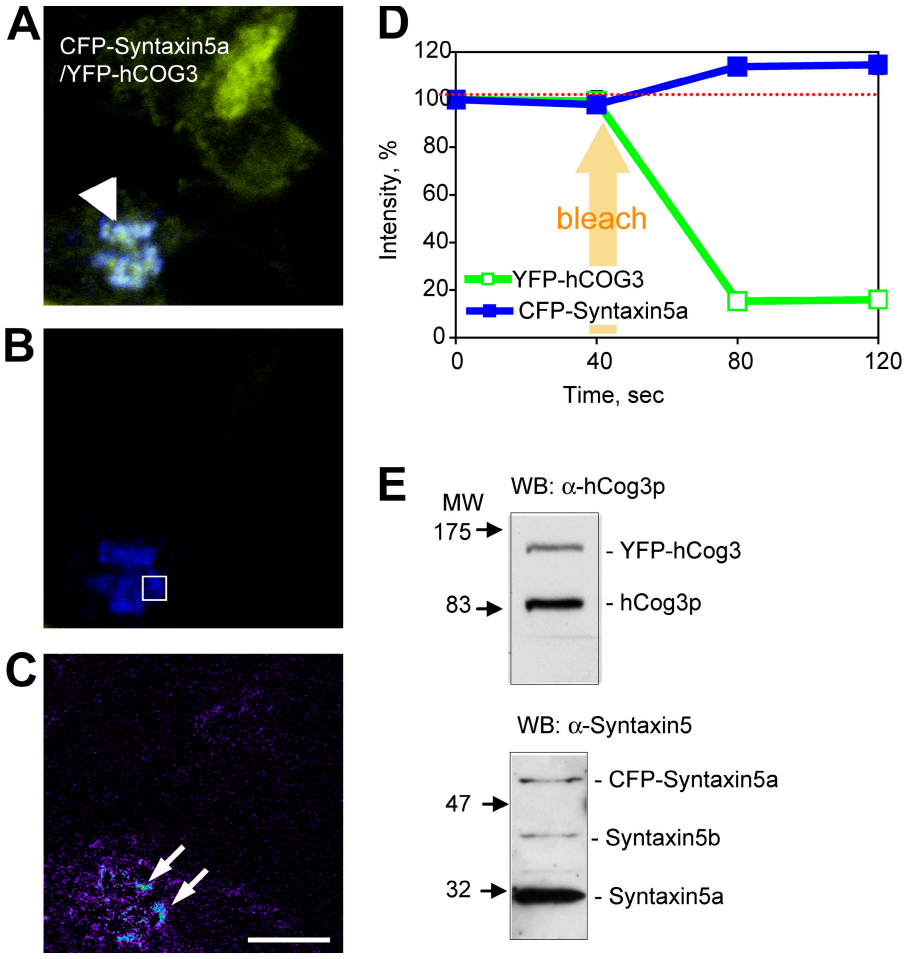

Figure 5. **FRET analysis of the COG–Syntaxin5a interaction in vivo.** (A–C) HeLa cells stably expressing YFP-hCog3 were transfected with the plasmid encoding CFP-Syntaxin5a. 24 h after transfection, physical interaction between CFP-Syntaxin5a and YFP-hCog3p was analyzed by the FRET protocol using a confocal microscope. CFP-Syntaxin5a signal before (A) and after (B) bleaching with a 514-nm laser (YFP bleach) and FRET ratio image (C) are shown using RGB (A and B) and rainbow (C) palettes. Bar, 10 μm. (D) CFP and YFP fluorescence before and after bleaching (n = 12) was calculated for the Golgi subregion (B, square). Both Golgi (A, arrowhead) and FRET-positive Golgi subregions (C, arrows) are indicated. Red dashed line is a baseline of CFP-Syntaxin5a signal before YFP-hCog3 bleaching. (E) Total cell lysates of HeLa cells stably expressing YFP-hCog3 or CFP-Syntaxin5a were analyzed by Western blot with antibodies indicated.

does not recognize Syntaxin5 within SNARE complexes, specifically labels Golgi ribbon in HeLa cells stably expressing GFP–*N*-acetylgalactosaminyltransferase-2 (GalNAcT2; Fig. 7, control, top, arrows). A fourfold decrease in 18C8 staining of perinuclear areas in the COG7 KD cells indicates accumulation of the uncomplexed form of Syntaxin5 in the Golgi region (Fig. 7, top, compare COG KD and control). A similar increase in staining for the uncomplexed form of Syntaxin5 is observed in COG3 and COG6 siRNA KD cells (unpublished data). The increase in 18C8 anti-Syntaxin5 staining is not because of the increased cellular level of Syntaxin5, because our previous experiments detected a decrease in a total cellular level of Syntaxin5 in both COG3 and COG7 KD cells (Shestakova et al., 2006). In contrast, siRNA KD of a trans-Golgi–localized small GTPase, Rab6, significantly reduces 18C8 immunostaining when compared with control cells (Fig. 7). Reduction of the uncomplexed Syntaxin5 signal in Rab6 KD cells might indicate that Rab6 is involved in the formation of the intra-Golgi transport carriers, which recycle uncomplexed SNARE molecules. This result is in agreement with our recent data, suggesting that Rab6 acts upstream of the COG complex in intra-Golgi trafficking because Rab6 KD prevents COG3 siRNA KD-induced fragmentation of Golgi (Sun et al., 2007).

Observed accumulation of uncomplexed Syntaxin5 might reflect a decrease in the formation of intra-Golgi Syntaxin5-containing SNARE complexes. To test this possibility, we performed native IP of the Golgi SNARE molecules in control, COG3, and COG7 KD cells. As the commercially available anti-GS15 antibody is not efficient for native IP (<5% recovery; unpublished data), we decided to use anti-GFP monoclonal 3E6 antibody to precipitate GS15-containing SNARE complexes in cells stably expressing GFP-GS15 (Fig. 8 A). As previously shown (Oka et al., 2004; Zolov and Lupashin, 2005), the protein level of GS15 is reduced in cells with the compromised COG complex function (Fig. 8 A, compare control and COG3 KD S20). Despite this, the IP of GFP-GS15 in COG3 KD cells is more efficient than in control cells and is accompanied by a significant (two- to threefold) reduction in the coisolation of GS28 and Syntaxin5a (Fig. 8 A, compare control and COG3 KD). A similar result is obtained after co-IP of GS28-containing SNARE complexes in COG7 KD cells (Fig. 8 B) with a twofold reduction in the coisolation of Syntaxin5a and a >10-fold reduction of GS15. Therefore, both COG3 and COG7 siRNA KD lead to a decrease in several Syntaxin5-containing intra-Golgi SNARE complexes.

Overexpression of the Cog4 N-terminal fragment destabilizes the Syntaxin5a–GS28 complex and disrupts Golgi structure

To test the functional relevance of the observed hCog4p–Syntaxin5a protein–protein interaction, we used an overexpression strategy.

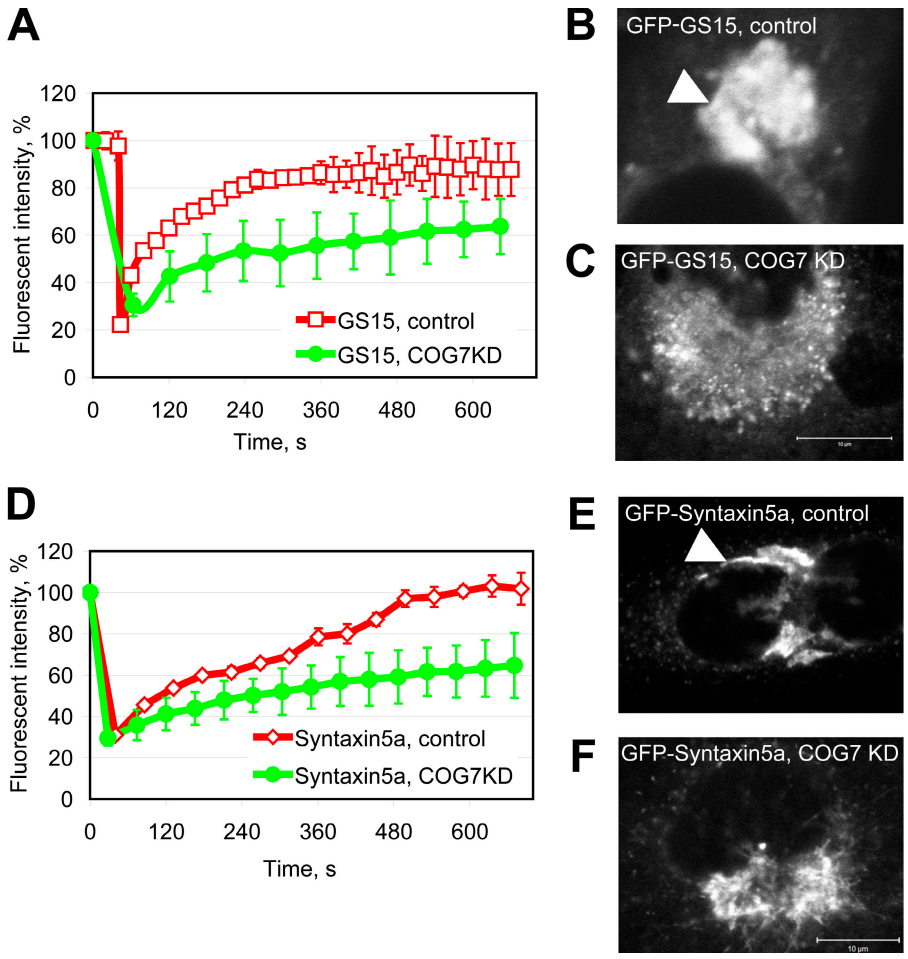

Figure 6. **Mobility of mammalian Golgi SNAREs is inhibited in COG7 KD cells.** HeLa cells stably expressing GFP-GS15 (A–C) or GFP-Syntaxin5a (D–F) were plated on a glass-bottom dish and transfected with scrambled (control) or COG7 siRNA. 72 h after transfection, FRAP was determined for each GFP-tagged SNARE molecule in perinuclear Golgi regions in control (red lines; $n = 10$) and COG7 siRNA KD (green lines; $n = 8$) cells in a CO_2-independent media at 25°C. Confocal images of control (B and E) and COG7 KD (C and F) cells are shown. Bars, 10 µm. Note that in control cells GFP-tagged proteins are correctly localized in the Golgi region (arrowheads). Error bars represent mean data.

HeLa cells stably expressing GFP-Syntaxin5a were transfected with either C-terminally myc-tagged full-length hCog4p or with its N-terminal 1–222-aa fragment (Fig. 9 A, lanes 2 and 3, respectively). A significant (7.3 ± 0.2%) amount of GS28 is coprecipitated with GFP-Syntaxin5a in control cells. We found that the Syntaxin5a–GS28 SNARE complex is disrupted in cells that overexpress 1–222 hCog4p (2.1 ± 0.5%) and to a similar extent (2.3 ± 0.3%) in cells that overexpress full-length hCog4p (Fig. 9 B, compare lanes 1′, 2′, and 3′). This effect is specific because the stability of the ER–Golgi SNARE complex that contains Bet1 and Syntaxin5a or b is not affected. The total level of GS28 in hCog4p(1–222)-myc–expressing cells is twofold (57 ± 9%) less than in control or full-length hCog4p-expressing cells. This finding is in agreement with a reduction in GOS-28 (GS28) protein level found in COG complex–deprived CHO cells (Oka et al., 2004). In 70% of cells ($n = 40$) that express hCog4p(1–222)-myc, GFP-Syntaxin5a is mislocalized from the perinuclear region into multiple fragmented membranes (Fig. 9 B, arrows). This is likely caused by the fragmentation of the entire Golgi because GalT staining reveals similar fragmentation (Fig. 9 B, compare GFP-Syntaxin5a and GalT). In contrast, Golgi fragmentation is observed only in 18% ($n = 66$) of control cells or cells expressing full-length hCog4p (unpublished data). The extent of Golgi fragmentation is proportional to the level of hCog4p(1–222)-myc expression, and the most severely disrupted Golgi structures are observed in cells that overexpress hCog4p(1–222)-myc (Fig. 9 B, double arrows).

Discussion

Several large cytosolic protein complexes are implicated in the regulation of membrane-trafficking events in eukaryotic cells (Oka and Krieger, 2005; Sztul and Lupashin, 2006). Defects in both the exocyst and COG complexes trigger an accumulation of nontethered vesicles, which are scattered throughout cytoplasm (Novick et al., 1980; Wuestehube et al., 1996; Zolov and Lupashin, 2005). Yeast exocyst-dependent vesicles are able to fuse with the plasma membrane (Novick et al., 1980). In mammalian cells, COG complex–dependent vesicles were shown to be functional intra-Golgi trafficking intermediates (Shestakova et al., 2006). Thus, these oligomeric complexes are proposed to mediate and/or control tethering of membrane transport intermediates (Whyte and Munro, 2002). Although vesicle-tethering complexes share little homology, they interact genetically and/or physically with members of the SNARE protein family. This suggests that tethers might regulate membrane trafficking through interaction with SNARE proteins.

In this paper, we studied the functional interaction between the COG complex and intra-Golgi SNARE molecules.

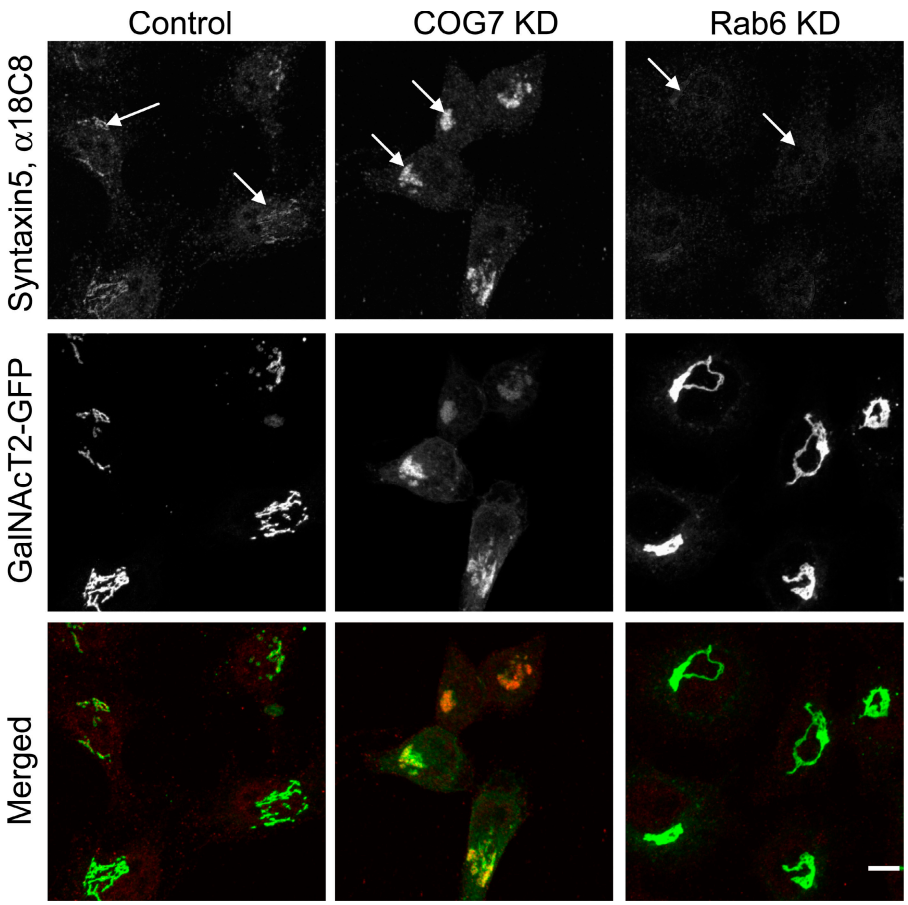

Figure 7. **Uncomplexed Golgi t-SNARE Syntaxin5 is accumulated in COG7 KD cells.** HeLa cells stably expressing GalNAcT2-GFP were treated with scrambled (control), COG7 siRNA (COG7 KD), and Rab6 siRNA (Rab6 KD) for 72 h. Cells were fixed and stained with primary 18C8 α-Syntaxin5 (Williams et al., 2004) and secondary Alexa 594 antibodies (red). Fluorescent confocal images were collected using a confocal microscope with identical parameters for the image acquisition. Note augmented uncomplexed Syntaxin5 staining in COG7 KD cells and decreased uncomplexed Syntaxin5 staining in Rab6 KD cells. Arrows, Syntaxin5 Golgi staining. Bar, 10 μm.

For the first time, we demonstrated that in mammalian and yeast cells the COG complex directly interacts with Golgi t-SNARE Syntaxin5a and Sed5p, respectively (Fig. 2, A–C ; and Fig. 4 A). The in vitro binding assay using purified yeast COG complex and SNARE molecules showed that the membrane-proximal α-helical domain of Sed5p (SNARE domain) is primarily involved in mediating interaction with the COG complex (Fig. 1, B–D). The same Sed5p SNARE domain was involved in mediating interactions with v-SNAREs during the formation of the SNARE complex (Sacher et al., 1997). Thus, it is important to determine if the COG complex discriminates between monomeric Sed5p and Sed5p within a SNARE complex. Rather surprisingly, the COG complex was shown to have a higher affinity for the preformed Sed5p-containing SNARE complex. In vitro binding assays determined that the yeast COG complex association is promiscuous and did not discriminate between preformed ER–Golgi [Sed5+Bos1+Sec22+Bet1] and intra-Golgi [Sed5+Gos1+Sec22+Sft1] SNARE complexes (Fig. 2, A–C). In contrast, the yeast COG complex preferentially coimmunoprecipitated with intra-Golgi SNARE molecules in vivo (Suvorova et al., 2002). This result suggested the existence of additional cellular factors that might restrict or regulate the interaction of the COG complex with a particular set of intra-Golgi SNAREs. The other explanation is that COG promiscuity in the binding experiments is caused by a substoichiometric level of yCog5p, 7p, and 8p observed in a purified yeast COG complex (Suvorova et al., 2002).

In addition, the yeast COG complex functionally participated in both ER–Golgi and intra-Golgi trafficking events as proposed in earlier studies (VanRheenen et al., 1998, 1999; Kim et al., 2001). The SNARE domain of Sed5p also interacted with Sec17p, a protein involved in the disassembly of the SNARE complex (Kosodo et al., 1998). It is tempting to hypothesize that the COG complex binding to Sed5p may compete with binding to the SNARE complex disassembly machinery (Sec17–Sec18 complex), thus prolonging the half-life of preassembled SNARE complexes.

Interestingly, overexpression of the major Sed5p-binding molecule Sly1p (Søgaard et al., 1994) inhibits the growth of the COG-deprived yeast cells (Fig. S4, available at http://www.jcb.org/cgi/content/full/jcb.200705145/DC1) and defects in the subunits of the COG complex are synthetically lethal when combined with the *sly1-ts* mutation (Ram et al., 2002). One plausible explanation for this phenomenon is that the COG complex and Sly1p have opposite regulatory roles in the t-SNARE cycle.

Importantly, we established that the interaction between the COG complex and Golgi t-SNARE Sed5p is evolutionarily conserved in yeast and mammalian cells. Syntaxin5a, the mammalian homologue of Sed5p, was coisolated with the COG complex (Figs. 3 A and 8 B). Syntaxin5a was the only SNARE molecule that interacted with the subunits of the COG complex in yeast two-hybrid assay (Fig. 4 A). In vivo coexpression experiments supported our yeast two-hybrid data and showed that >10% of an N-terminal hCog4 polypeptide is recovered with Syntaxin5a (Fig. 4, B and C). The hCog4–Syntaxin5a interaction

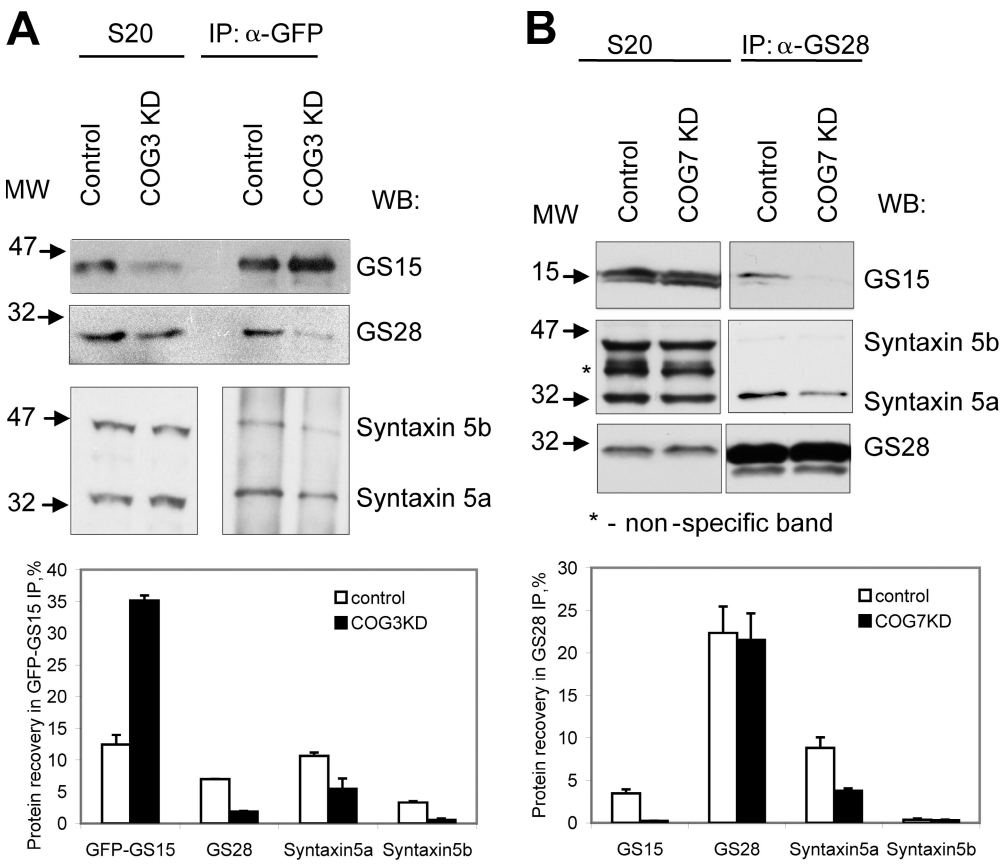

Figure 8. **Golgi SNARE complex is destabilized in Cog3p- and Cog7p-depleted cells.** (A) HeLa cells stably expressing GFP-GS15 were treated with scrambled (control) and COG3 siRNA for 72 h. GFP-GS15–containing SNARE complexes were precipitated from the 1% Triton X-100–solubilized cell lysates using anti-GFP antibody. 10% of the cell lysate (S20) and 100% of immunoprecipitate were immunoblotted with antibodies as indicated. Note that polyclonal anti-Syntaxin5 antibodies recognize both short (Syntaxin5a) and long (Syntaxin5b) isoforms of Syntaxin5 proteins. The results were plotted in a bar graph. (B) HeLa cells were treated with scrambled (control) and COG7 siRNA for 72 h. GS28-containing SNARE complexes were precipitated from the 1% Triton X-100–solubilized cell lysates using anti-GS28 antibody. 10% of the cell lysates (S20) and 100% of the immunoprecipitate (IP) were immunoblotted with antibodies as indicated. Error bars represent mean intensity of protein bands, calculated with ImageJ software, from three independent experiments

is functionally relevant because overexpression of the 1–222 hCog4 N-terminal polypeptide interfered with the formation of intra-Golgi SNARE complex and destabilized GS28 protein causing extensive Golgi fragmentation (Fig. 9 B). It is also possible that degradation of GS28 in hCog4p(1–222)-expressing cells is partially caused by the disruption of Golgi ribbon, which is not the case in cells overexpressing full-length hCog4p. We have observed previously that in COG3 siRNA KD cells, Golgi fragmentation was associated with increased degradation of GS28 (Zolov and Lupashin, 2005). The COG subunits, which showed an interaction with Syntaxin5a, hCog4p, and hCog6p, are evolutionarily conserved (Whyte and Munro, 2002). The N-terminal domain of hCog4p (aa 1–222) is homologous to the corresponding domain of yCog4p with a 47% similarity. Notably, yCog4p (TFI3) demonstrated the strongest in vivo interaction with Sed5p (Fig. 7 in Suvorova et al., 2002), and bacterially expressed yCog4p and Sed5p interacted in the in vitro binding studies (unpublished data). In addition, the myc-tagged N-terminal domain of yCog4p(1–250) is coprecipitated with Sed5p in wild-type yeast and even more efficiently in *sed5-ts* cells (Fig. S5 A, available at http://www.jcb.org/cgi/content/full/jcb.200705145/DC1). In a later case, GAL promoter–driven overexpression of yCog4p inhibited growth of *sed5-ts* cells (Fig. S5 B). Collectively, these data support the hypothesis that the function of the COG complex in membrane traffic is mediated via interaction with SNARE proteins.

How could direct binding of the COG complex modulate the function of a SNARE complex? Association of the large COG complex with the specific trans-SNARE bundle could transiently stabilize v- or t-SNARE interaction by preventing SNARE complex dissociation by the SNAP–NSF (Sec17–Sec18 in yeast) chaperone complex. The exact number of SNARE complexes required for one membrane fusion event is unknown. Independent binding of two COG complex subunits, hCog4p and 6p, to Syntaxin5a may facilitate an arrangement of several SNARE complexes into the fusogenic super complex. Additionally, the COG complex may potentially directly stimulate individual trans-SNARE complex formation, although our attempts to influence the rate of SNARE complex formation in vitro by addition of the purified COG complex were inconclusive (unpublished data).

In conclusion, we propose a possible model for the stepwise involvement of oligomeric tethers and SNAREs in vesicle docking during Golgi vesicular trafficking.

First, a long rod-like coiled coil tether, like p115 (Uso1p in yeast), binds to vesicles and to the target membranes, establishing

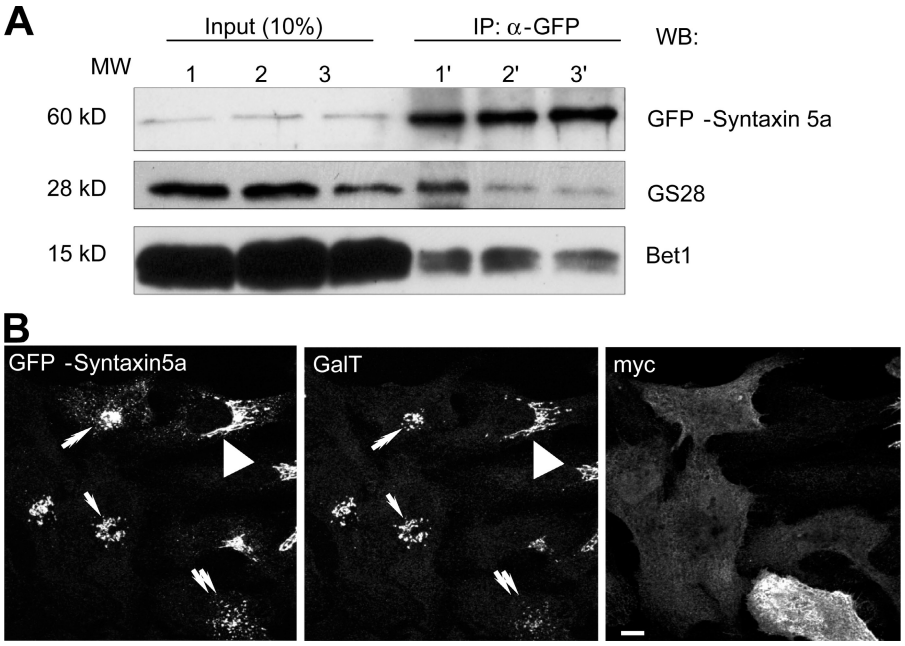

Figure 9. **Overexpression of the Syntaxin5a-interacting domain of hCog4p affects Golgi morphology and stability of intra-Golgi SNARE complex.** HeLa cells stably expressing GFP-Syntaxin5a were transfected with plasmids encoding mRFP, hCog4-myc, or hCog4(1–222)-myc. (A) GFP-Syntaxin5a–containing SNARE complexes were precipitated from the Triton X-100–solubilized cell lysates using anti-GFP antibody. Lanes 1 and 1′, transfected with mRFP; lanes 2 and 2′, transfected with full-length hCog4-myc; and lanes 3 and 3′, transfected with hCog4(1–222)-myc. 10% of the cell lysates (Input) and 100% of the immunoprecipitate (IP) were immunoblotted with antibodies as indicated. (B) 24 h after transfection with hCog4(1–222)-myc, cells were fixed and stained with primary anti-GalT monoclonal and anti-myc polyclonal antibodies, and then with secondary anti–mouse-HiLyte Fluor 647 and anti–rabbit-HiLyte Fluor 555, respectively. Fluorescent confocal images were collected using a confocal microscope. Note solid Golgi ribbon staining in untransfected cells (arrowheads), fragmented perinuclear Golgi in cells that moderately express hCog4(1–222)-myc (arrows), and severely fragmented Syntaxin5a and GalT staining in cells that overexpress hCog4(1–222)-myc (double arrows). Bar, 10 μm.

initial loose interaction. This binding is transient because p115 rapidly ($t_{1/2}$ of ~10 s) exchanges between cytosolic and membrane fractions (Brandon et al., 2006). At this step, a coiled coil tether interacts with Rab and SNARE molecules. Second, an oligomeric tether, like the COG complex, binds to the vesicles, establishing a firm docking complex. The COG complex operates on the cis/medial Golgi cisternae and is stably associated with the membranes (hCog3p resident time on the Golgi, $t_{1/2}$ of >5 min; unpublished data), preferentially localizing to the tips and rims of the Golgi cisternae (Vasile et al., 2006). Third, a SNARE-related domain of p115 stimulates the specific zippering of Golgi SNAREpins (Shorter et al., 2002). Simultaneously, bound COG complex stabilizes SNARE complexes. Finally, vesicles fuse with the target membrane and the cis-SNARE complexes are dissociated in the NSF-dependent reaction, allowing recycling of both coiled coil and oligomeric tethers.

In support of this model, both p115 and the COG complex are required at the same stage of the in vitro reaction that reconstitutes efficient intercisternal transport within the Golgi stack (Waters et al., 1992; Walter et al., 1998) and both interact with the same set of Golgi SNARE molecules (Shorter et al., 2002; Suvorova et al., 2002). Functional in vivo interactions between the COG complex and Golgi SNARE molecules are transient, restricted to active trafficking zones (Fig. 5), and most likely regulated by additional binding partners (Rabs, coat proteins, etc.). In addition to binding to p115, the COG complex also interacts with the p115 binding partner GM130 (Fig. 3 A). In yeast, temperature-sensitive *uso1-1* and *cog2-ts* (*sec35-1*) mutations are synthetically lethal (VanRheenen et al., 1998) and the overexpression of Uso1p suppresses growth defects in COG3-deficient cells (VanRheenen et al., 1999). This observation, together with recent findings that the COG complex directly interacts with p115 (Sohda et al., 2007), supports the hypothesis that coiled coil tethers and large oligomeric tethering factors actively cooperate during membrane tethering, docking, and fusion via interaction with SNARE molecules (Sztul and Lupashin, 2006).

Both the COG complex and the Golgi SNARE proteins are expected to participate in several distinct membrane-trafficking steps. The discovery of the evolutionarily conserved direct functional interaction between the oligomeric tethering factor and SNARE proteins provides new insight in the membrane-trafficking field. It will be beneficial to further decipher tether–SNARE–Rab interactions regulating specific vesicle–membrane interactions.

Materials and methods

Reagents and antibodies

Antibodies for Western blotting (WB), IF, and IP were obtained either from commercial sources or as gifts from individual investigators, or they were generated by us. Antibodies (and their dilutions) are as follows: rabbit affinity-purified anti-yCog1p (WB 1:100), yCog2p (WB 1:500), and yCog3p (WB 1:500; IF 1:100); anti-hCog3p (WB 1:1,000) and hCog8p (WB 1:3,000); p115 (WB 1:1,000); mouse anti-GM130 (WB 1:500; IF 1:250); anti–human GS28 (WB 1:500; IF 1:100; BD Biosciences); anti-Bet1 (WB 1:200; BD Biosciences); anti–protein disulfide isomerase (WB 1:5,000; IF 1:200; IP 1:2,000; Affinity BioReagents); anti–rat GS28 (WB 1:500; Assay Designs); anti-GAPDH (WB 1:1,000; Ambion); anti-GFP clone 3E6 (Invitrogen); and anti-Syntaxin5 18C8 (IF 1:100; gift from J. Hay, University of Montana, Missoula, MT). Secondary anti–rabbit-HRP and anti–mouse-HRP for WB were obtained from Jackson ImmunoResearch Laboratories. Secondary anti–rabbit Alexa 594 was obtained from Invitrogen and anti–rabbit-HiLyte Fluor 555 and anti–mouse HiLyte Fluor 647 were obtained from AnaSpec, Inc.

The reagent used was protein G–Sepharose (EMD).

Mammalian cell culture

HeLa cells were cultured in DME/F-12 media supplemented with 15 mM Hepes, 2.5 mM L-glutamine, 5% FBS, 100 U/ml penicillin G, 100 μg/ml streptomycin, and 0.25 μg/ml amphotericin B. Cells were grown at 37°C and 5% CO_2 in a humidified chamber. HeLa cells stably expressing GalNAcT2-GFP were a gift from B. Storrie (University of Arkansas for Medical

Sciences, Little Rock, AR). All cell culture media and sera were obtained from Invitrogen.

HeLa stable cell lines expressing mammalian COG and SNARE constructs

Rat Syntaxin5a in pEGFP-C1 and pECFP-C1 vectors were a gift from R. Duden (Royal Holloway University of London, Egham, UK). Rat Syntaxin6 and rat membrin in pECFP-C1 vector were a gift from R. Scheller (Stanford University, Palo Alto, CA). Plasmid encoding RFP (mRFP) was a gift from R.S. Tsien (University of California, San Diego, San Diego, CA). cDNAs encoding human Cog6p and human GS15 were purchased from Open Biosystems. All constructs used in this study were verified by sequencing.

HeLa-YFP-hCog3p, HeLa-GFP-Syntaxin5a, and HeLa-GFP-GS15 stable cell lines were obtained by transfecting HeLa cells with plasmids encoding either YFP-hCog3p (Suvorova et al., 2001), EGFP-Syntaxin5a, or EGFP-GS15, followed by the selection for G418 resistance. Single cell–derived clones were screened for YFP-hCog3p, GFP-Syntaxin5a, and GFP-GS15 expression by Western blot with anti-GFP antibody. Selected stable colonies expressed GFP-tagged molecules at the level of the endogenous proteins.

In vitro binding assay

The COG complex was purified from TAP-yCog2 cells as described previously (Suvorova et al., 2002). The purified yeast COG complex used in in vitro experiments contains stoichiometric levels of yCog1–4 and 6 and substoichiometric levels of Cog5, 7, and 8 (Suvorova et al., 2002). Immunoblotting detected all eight COG subunits in TAP-yCog2–purified COG complex (Fotso et al., 2005). GST-tagged Sft1p, Bet1p, Sec22p, Sed5p, and Sso1p were generated by subcloning the cDNA for the cytoplasmic domains of the corresponding yeast proteins into a pGEX4T vector (GE Healthcare). Plasmids encoding GST-tagged domains of Sed5p (Kosodo et al., 1998) were a gift from K. Yoda (University of Tokyo, Tokyo, Japan). Proteins were expressed in *Escherichia coli* XL-10 cells and affinity purified on glutathione-Sepharose beads (GE Healthcare) according to the manufacturer's instructions. His6-Sec22p, His6-Sed5p, and yeast expression plasmids encoding GST-Sly1p and GST-Sly1-20 were described previously (Sapperstein et al., 1996; Lupashin and Waters, 1997; Lupashin et al., 1997). Plasmids encoding His6-Gos1p and His6-Bos1p (Tsui and Banfield, 2000) were a gift from D. Banfield (The Hong Kong University of Science and Technology, Hong Kong, China). His-tagged proteins were purified on TALON resin (Clontech Laboratories, Inc.) as described previously (Fotso et al., 2005). SNARE complexes were formed by mixing 1 mg/ml each of purified GST- and His-tagged proteins in TBS for 18 h on ice. Prolonged (18 h) incubation of purified proteins on ice did not significantly change their binding properties. SNARE complexes were first isolated on TALON resin (Clontech Laboratories, Inc.), and then by the glutathione-Sepharose affinity purification. The composition of SNARE complexes was verified by immunoblotting. 10 μl of glutathione-Sepharose beads with prebound single SNARE protein or SNARE complexes (each containing 5 pmol of Sed5 protein) were mixed with purified COG complex in B88 buffer and incubated for 3 h at 4°C. GST-tagged and coprecipitated proteins were eluted in 20 mM of reduced glutathione, pH 7.5. Interactions were determined by Western blot as described previously (Suvorova et al., 2002).

Yeast two-hybrid assay

The following constructs were used in yeast two-hybrid assay: the eight (1–8) subunits of mammalian COG complex cloned as C-terminal fusion constructs with Gal4 AD (prey) or BD (bait) by recombination cloning in yeast. All plasmids encoding COG subunit fusions (Ungar et al., 2005) as well as empty vectors pGAD-C1 (AD) and pGBDU-C1 (BD) were a gift from D. Ungar (Princeton University, Princeton, NJ). Chimera SNARE molecules were constructed as the C-terminal fusions with GAL4 AD and BD without the transmembrane domain. Syntaxin5a H3 and H1H2 domains were fused with GAL4 AD.

DNA encoding mammalian (human and rat) Syntaxin5a, Syntaxin6, GS15, GS28, membrin, and Bet1 were purchased from Open Biosystems. PCRs of the sequence encoding the SNARE's cytoplasmic domain were performed using corresponding sense primers with either EcoRI (for Syntaxin5a and 6) or BamHI (GS15 and 28) sites and antisense primers with either XhoI or SalI sites. The PCR products were digested with EcoRI–XhoI or BamHI–Xho1 and ligated into pGAD-C1 and pGBDU-C1 digested with BamHI and SalI.

The Gal4 two-hybrid system was used as previously described (James et al., 1996). Reporter strains of opposite mating types LY612 (Mat a) and LY613 (Mat α; trp1–901 leu2–3,112 ura3–52 his3–200 gal4 Δgal80Δ LYS2::GAL1-HIS3 GAL2-ADE2 met2::GAL7-lacZ) were transformed with bait and prey fusion constructs. The growth of independent transformants was assessed on media lacking leucine (prey fusions) and uracil (bait fusions). Diploid yeasts containing combinations of the human COG subunits 1–8 and SNAREs, as well as empty vectors (negative controls) and pairwise combinations of human COG4/5, 2/4, and 5/7 (positive controls; Ungar et al., 2005) were created by mass mating. After mass mating, yeast diploids were selected on −LEU/−URA plates. Diploids were grown in liquid −Leu/−Ura medium to the same optical density (D_{600} = 0.8) and titrated 1:10, 1:100, 1:1,000, and 1:10,000 in ddH_2O. 5 μl of each dilution was applied on a selective medium lacking adenine, histidine, and leucine/uracil, incubated at 30°C for 72 h, and scored for growth. Expression of all hybrid molecules was verified by immunoblotting. The relative stringency of direct protein–protein interaction was estimated by growth assay on agar plates lacking either histidine (−HIS; leaky regulation, suitable for weak protein–protein interaction) or adenine (−ADE; high stringency regulation, suitable for strong protein–protein interaction).

siRNA

Human COG3 and 7 were targeted with siRNA duplexes as described previously (Zolov and Lupashin, 2005; Shestakova et al., 2006). Cells were transfected with Oligofectamine (Invitrogen) twice in each 24-h period according to the protocol by Invitrogen. For IF microscopy and WB, HeLa cells were grown in 35-mm dishes (on coverslips for IF) at 60% confluence, washed with PBS, and lysed in 2% SDS 72 h after COG3 or COG7 siRNA KD.

IP and fluorescence microscopy

Rat liver Golgi membranes were prepared as described previously (Zolov and Lupashin, 2005).

For IP, HeLa cells and rat liver Golgi membranes were lysed on ice in 1 ml DPBST buffer (DPBS, 1% Triton X-100, and protease inhibitor cocktail). Lysates were incubated with 30 μl of protein A–Sepharose CL-4B beads, and then mixed by gentle inversion for 1 h on ice and clarified by centrifugation at 20,000 *g* for 10 min. Supernatants were transferred to new eppendorf tubes with 2 μg of antibody and incubated overnight on ice. The samples were then clarified by centrifugation as with the lysates, and 20 μl of protein G–Agarose beads slurry (50%) was added to each tube and incubated for 2 h with gentle inversion in a cold room. The beads were then washed four times with TBST and transferred to new eppendorf tubes, resuspended in 50 μl of 1X sample buffer, and heated for 5 min at 95°C to elute the bound proteins.

For IF, cells were grown on coverslips 1 d before transfection. 72 h after siRNA transfection, cells were fixed and stained with antibodies as previously described (Jiang and Storrie, 2005; Shestakova et al., 2006). Widefield microscopy and imaging were performed with a microscope (200M; Zeiss Axiovert; Carl Zeiss, Inc.) fitted with CARV II accessory (BD Biosciences) mounted to the sideport. A 63× 1.4 NA oil objective was used and images were captured by a camera (Retiga EXi; QImaging). Image acquisition was controlled with IPlab 3.9.5 software (Apple; Scanalytics). Images were cropped with Photoshop 6.0 (Adobe) software. Image stacks (8 × 0.25 μm) for the Golgi apparatus were collected through the entire cell depth and compressed into a single plane using IPLab.

Coexpression of GFP-Syntaxin5a and myc-tagged COG subunits in HeLa cells

Plasmids expressing 3xmyc C-terminally tagged Cog4p and Cog6p were a gift from S. Munro (University of Cambridge, Cambridge, UK) and were described in Whyte and Munro (2001). DNA constructs encoding 3xmyc C-terminally tagged hCog4(1–150) and hCog4(1–222) were made by PCR and verified by sequencing. For IF experiments, HeLa cells were grown on glass coverslips and cotransfected with plasmids encoding either EGFP or EGFP-Syntaxin5a or myc-tagged COG complex subunits. 36 h after transfection, cells were fixed and stained with the antibodies as previously described (Jiang and Storrie, 2005; Shestakova et al., 2006). For co-IP experiments, HeLa cells grown on 60-mm dishes were transfected as the HeLa cells. 36 h after transfection, cells were lysed and protein complexes were immunoprecipitated (as described in IP and fluorescence microscopy) with anti-myc or anti-GFP antibodies and analyzed by immunoblotting.

Live cell imaging

HeLa cells grown on glass coverslips to 50–60% confluence in 35-mm dishes were transfected with the respective plasmids and imaged after 24 h in a silicon gasket–sealed chamber. During the imaging period, the culture medium was buffered with 25 mM Hepes and the microscope stage was

maintained between 32 and 37°C. We use the 63× 1.4NA oil objective of a laser-inverted microscope (LSM510; Carl Zeiss, Inc.) outfitted with confocal optics for image acquisition. Image acquisition was controlled with LSM510 software (Release Version 4.0 SP1; Carl Zeiss, Inc.).

FRET and FRAP

A laser confocal microscope (LSM 510; Carl Zeiss, Inc) was used for FRET and FRAP. CFP-Syntaxin5a/YFP-hCog3 FRET signal was measured in HeLa cells stably expressing YFP-hCog3 and transiently expressing CFP-Syntaxin5a. Protein level of CFP-Syntaxin5a expression was measured by immunoblotting to optimize expression to that of endogenous Syntaxin5a. A similar method was used to measure FRET signal for CFP-hCog6/YFP-hCog3 and CFP-Syntaxin6/YFP-hCog3 pairs. Cells ($n = 20$) with the Golgi-localized CFP-Syntaxin5a were imaged. For the acceptor-bleached protocol, cells were excited at 40-s intervals at 458 nm for CFP detection and at 514 nm for YFP detection. After two excitation cycles, YFP was bleached at 514 nm. This procedure resulted in >90% of YFP photobleached within 10 s. The ratio of CFP-Syntaxin5a fluorescence recovery before and after photobleaching was used as a measure of the CFP-donor/YFP-acceptor FRET signal.

For FRAP, a single prebleach image was obtained, followed by a 10-s photobleach with the 488-nm argon laser. Post-bleach images were obtained every 30 s. Each round of scanning took 10 s in the 512 × 512 format. Every image was a mean of four frames. Images (in TIFF format) were analyzed by ImageJ (National Institutes of Health; http://rsb.info.nih.gov/ij/download.html) and fluorescence intensities were analyzed using Excel (Microsoft). Graphs and statistical analyses were performed in Excel.

SDS-PAGE and WB

SDS-PAGE and WB were performed as described previously (Suvorova et al., 2002). A signal was detected using an ECL reagent kit (PerkinElmer) and quantified using ImageJ.

Online supplemental material

Fig. S1 provides colocalization images of yeast Cog3p and Sed5p. Fig. S2 shows converse yeast two-hybrid assay of BD-Syntaxin5a with AD-hCog1–8, as well as AD-hCog4 with SNARE and H1 + H2 domains of BD-Syntaxin5a. Fig. S3 shows in vivo FRET analysis of the positive control between hCog3p–hCog6p pair and the negative control between hCog3p–Syntaxin6 pair. Fig. S4 shows that overexpression of Sed5p-interacting protein Sly1p is toxic in yeast cells with a defective COG complex. Fig. S5 demonstrates that the N-terminal Sed5p BD of yeast yCog4p is coimmunoprecipitated with Sed5p. Online supplemental material is available at http://www.jcb.org/cgi/content/full/jcb.200705145/DC1.

We are very thankful to M. Babst, D. Banfield, R. Duden, J. Hay, F. Hughson, R. Scheller, B. Storrie, E. Sztul, D. Ungar, K. Yoda, and others who provided reagents and critical reading of the manuscript.

This work was supported by grants from the National Science Foundation (MCB-0234822 and MCB-0645163) and the Mizutani Foundation for Glycoscience to V. Lupashin and was initiated with support from the Arkansas Bioscience Institute. A. Shestakova was partially supported by the American Heart Association (grant 0530210N.3) to M. Babst.

Submitted: 23 May 2007
Accepted: 19 November 2007

References

Bonifacino, J.S., and B.S. Glick. 2004. The mechanisms of vesicle budding and fusion. *Cell*. 116:153–166.

Bracher, A., and W. Weissenhorn. 2002. Structural basis for the Golgi membrane recruitment of Sly1p by Sed5p. *EMBO J.* 21:6114–6124.

Brandon, E., T. Szul, C. Alvarez, R. Grabski, R. Benjamin, R. Kawai, and E. Sztul. 2006. On and off membrane dynamics of the endoplasmic reticulum-Golgi tethering factor p115 in vivo. *Mol. Biol. Cell*. 17:2996–3008.

Fotso, P., Y. Koryakina, O. Pavliv, A.B. Tsiomenko, and V.V. Lupashin. 2005. Cog1p plays a central role in the organization of the yeast conserved oligomeric golgi complex. *J. Biol. Chem.* 280:27613–27623.

Foulquier, F., E. Vasile, E. Schollen, N. Callewaert, T. Raemaekers, D. Quelhas, J. Jaeken, P. Mills, B. Winchester, M. Krieger, et al. 2006. Conserved oligomeric Golgi complex subunit 1 deficiency reveals a previously uncharacterized congenital disorder of glycosylation type II. *Proc. Natl. Acad. Sci. USA*. 103:3764–3769.

Fridmann-Sirkis, Y., H.M. Kent, M.J. Lewis, P.R. Evans, and H.R. Pelham. 2006. Structural analysis of the interaction between the SNARE Tlg1 and Vps51. *Traffic*. 7:182–190.

Guo, W., D. Roth, C. Walch-Solimena, and P. Novick. 1999. The exocyst is an effector for Sec4p, targeting secretory vesicles to sites of exocytosis. *EMBO J.* 18:1071–1080.

James, P., J. Halladay, and E.A. Craig. 1996. Genomic libraries and a host strain designed for highly efficient two-hybrid selection in yeast. *Genetics*. 144:1425–1436.

Jiang, S., and B. Storrie. 2005. Cisternal rab proteins regulate Golgi apparatus redistribution in response to hypotonic stress. *Mol. Biol. Cell*. 16:2586–2596.

Jones, S., C. Newman, F. Liu, and N. Segev. 2000. The TRAPP complex is a nucleotide exchanger for Ypt1 and Ypt31/32. *Mol. Biol. Cell*. 11:4403–4411.

Kim, D.W., M. Sacher, A. Scarpa, A.M. Quinn, and S. Ferro-Novick. 1999. High-copy suppressor analysis reveals a physical interaction between Sec34p and Sec35p, a protein implicated in vesicle docking. *Mol. Biol. Cell*. 10:3317–3329.

Kim, D.W., T. Massey, M. Sacher, M. Pypaert, and S. Ferro-Novick. 2001. Sgf1p, a new component of the Sec34p/Sec35p complex. *Traffic*. 2:820–830.

Kingsley, D.M., K.F. Kozarsky, M. Segal, and M. Krieger. 1986. Three types of low density lipoprotein receptor-deficient mutant have pleiotropic defects in the synthesis of N-linked, O-linked, and lipid-linked carbohydrate chains. *J. Cell Biol.* 102:1576–1585.

Kosodo, Y., Y. Noda, and K. Yoda. 1998. Protein-protein interactions of the yeast Golgi t-SNARE Sed5 protein distinct from its neural plasma membrane cognate syntaxin 1. *Biochem. Biophys. Res. Commun.* 250:212–216.

Kubota, Y., M. Sano, S. Goda, N. Suzuki, and K. Nishiwaki. 2006. The conserved oligomeric Golgi complex acts in organ morphogenesis via glycosylation of an ADAM protease in *C. elegans*. *Development*. 133:263–273.

Liu, Y., and C. Barlowe. 2002. Analysis of Sec22p in endoplasmic reticulum/Golgi transport reveals cellular redundancy in SNARE protein function. *Mol. Biol. Cell*. 13:3314–3324.

Lupashin, V.V., and M.G. Waters. 1997. t-SNARE activation through transient interaction with a Rab-like guanosine triphosphatase. *Science*. 276:1255–1258.

Lupashin, V.V., I.D. Pokrovskaya, J.A. McNew, and M.G. Waters. 1997. Characterization of a novel yeast SNARE protein implicated in Golgi retrograde traffic. *Mol. Biol. Cell*. 8:2659–2676.

Novick, P., C. Field, and R. Schekman. 1980. Identification of 23 complementation groups required for post-translational events in the yeast secretory pathway. *Cell*. 21:205–215.

Oka, T., and M. Krieger. 2005. Multi-component protein complexes and Golgi membrane trafficking. *J. Biochem. (Tokyo)*. 137:109–114.

Oka, T., D. Ungar, F.M. Hughson, and M. Krieger. 2004. The COG and COPI complexes interact to control the abundance of GEARs, a subset of Golgi integral membrane proteins. *Mol. Biol. Cell*. 15:2423–2435.

Oka, T., E. Vasile, M. Penman, C.D. Novina, D.M. Dykxhoorn, D. Ungar, F.M. Hughson, and M. Krieger. 2005. Genetic analysis of the subunit organization and function of the conserved oligomeric golgi (COG) complex: studies of COG5- and COG7-deficient mammalian cells. *J. Biol. Chem.* 280:32736–32745.

Peng, R., A. De Antoni, and D. Gallwitz. 2000. Evidence for overlapping and distinct functions in protein transport of coat protein Sec24p family members. *J. Biol. Chem.* 275:11521–11528.

Pfeffer, S.R. 2001. Rab GTPases: specifying and deciphering organelle identity and function. *Trends Cell Biol.* 11:487–491.

Price, A., D. Seals, W. Wickner, and C. Ungermann. 2000. The docking stage of yeast vacuole fusion requires the transfer of proteins from a cis-SNARE complex to a Rab/Ypt protein. *J. Cell Biol.* 148:1231–1238.

Ram, R.J., B. Li, and C.A. Kaiser. 2002. Identification of sec36p, sec37p, and sec38p: components of yeast complex that contains sec34p and sec35p. *Mol. Biol. Cell*. 13:1484–1500.

Rieder, S.E., and S.D. Emr. 1997. A novel RING finger protein complex essential for a late step in protein transport to the yeast vacuole. *Mol. Biol. Cell*. 8:2307–2327.

Sacher, M., S. Stone, and S. Ferro-Novick. 1997. The synaptobrevin-related domains of Bos1p and Sec22p bind to the syntaxin-like region of Sed5p. *J. Biol. Chem.* 272:17134–17138.

Sapperstein, S.K., V.V. Lupashin, H.D. Schmitt, and M.G. Waters. 1996. Assembly of the ER to Golgi SNARE complex requires Uso1p. *J. Cell Biol.* 132:755–767.

Shestakova, A., S. Zolov, and V. Lupashin. 2006. COG complex-mediated recycling of Golgi glycosyltransferases is essential for normal protein glycosylation. *Traffic*. 7:191–204.

Shorter, J., M.B. Beard, J. Seemann, A.B. Dirac-Svejstrup, and G. Warren. 2002. Sequential tethering of Golgins and catalysis of SNAREpin assembly by the vesicle-tethering protein p115. *J. Cell Biol.* 157:45–62.

Siniossoglou, S., and H.R. Pelham. 2001. An effector of Ypt6p binds the SNARE Tlg1p and mediates selective fusion of vesicles with late Golgi membranes. *EMBO J.* 20:5991–5998.

Sivaram, M.V., J.A. Saporita, M.L. Furgason, A.J. Boettcher, and M. Munson. 2005. Dimerization of the exocyst protein Sec6p and its interaction with the t-SNARE Sec9p. *Biochemistry*. 44:6302–6311.

Søgaard, M., K. Tani, R.R. Ye, S. Geromanos, P. Tempst, T. Kirchhausen, J.E. Rothman, and T. Söllner. 1994. A rab protein is required for the assembly of SNARE complexes in the docking of transport vesicles. *Cell*. 78:937–948.

Sohda, M., Y. Misumi, S. Yoshimura, N. Nakamura, T. Fusano, S. Ogata, S. Sakisaka, and Y. Ikehara. 2007. The interaction of two tethering factors, p115 and COG complex, is required for Golgi integrity. *Traffic*. 8:270–284.

Stroupe, C., K.M. Collins, R.A. Fratti, and W. Wickner. 2006. Purification of active HOPS complex reveals its affinities for phosphoinositides and the SNARE Vam7p. *EMBO J.* 25:1579–1589.

Sun, Y., A. Shestakova, L. Hunt, S. Sehgal, V. Lupashin, and B. Storrie. 2007. Rab6 regulates both ZW10/RINT-1 and conserved oligomeric golgi complex-dependent Golgi trafficking and homeostasis. *Mol. Biol. Cell*. 18:4129–4142.

Suvorova, E.S., R.C. Kurten, and V.V. Lupashin. 2001. Identification of a human orthologue of Sec34p as a component of the cis-Golgi vesicle tethering machinery. *J. Biol. Chem.* 276:22810–22818.

Suvorova, E.S., R. Duden, and V.V. Lupashin. 2002. The Sec34/Sec35p complex, a Ypt1p effector required for retrograde intra-Golgi trafficking, interacts with Golgi SNAREs and COPI vesicle coat proteins. *J. Cell Biol.* 157:631–643.

Sztul, E., and V. Lupashin. 2006. Role of tethering factors in secretory membrane traffic. *Am. J. Physiol. Cell Physiol.* 290:C11–C26.

Tsui, M.M., and D.K. Banfield. 2000. Yeast Golgi SNARE interactions are promiscuous. *J. Cell Sci.* 113:145–152.

Tsui, M.M., W.C. Tai, and D.K. Banfield. 2001. Selective formation of Sed5p-containing SNARE complexes is mediated by combinatorial binding interactions. *Mol. Biol. Cell*. 12:521–538.

Ungar, D., and F.M. Hughson. 2003. SNARE protein structure and function. *Annu. Rev. Cell Dev. Biol.* 19:493–517.

Ungar, D., T. Oka, E.E. Brittle, E. Vasile, V.V. Lupashin, J.E. Chatterton, J.E. Heuser, M. Krieger, and M.G. Waters. 2002. Characterization of a mammalian Golgi-localized protein complex, COG, that is required for normal Golgi morphology and function. *J. Cell Biol.* 157:405–415.

Ungar, D., T. Oka, E. Vasile, M. Krieger, and F.M. Hughson. 2005. Subunit architecture of the conserved oligomeric Golgi complex. *J. Biol. Chem.* 280:32729–32735.

VanRheenen, S.M., X. Cao, V.V. Lupashin, C. Barlowe, and M.G. Waters. 1998. Sec35p, a novel peripheral membrane protein, is required for ER to Golgi vesicle docking. *J. Cell Biol.* 141:1107–1119.

VanRheenen, S.M., X. Cao, S.K. Sapperstein, E.C. Chiang, V.V. Lupashin, C. Barlowe, and M.G. Waters. 1999. Sec34p, a protein required for vesicle tethering to the yeast Golgi apparatus, is in a complex with Sec35p. *J. Cell Biol.* 147:729–742.

Vasile, E., T. Oka, M. Ericsson, N. Nakamura, and M. Krieger. 2006. IntraGolgi distribution of the Conserved Oligomeric Golgi (COG) complex. *Exp. Cell Res.* 312:3132–3141.

von Mollard, G.F., S.F. Nothwehr, and T.H. Stevens. 1997. The yeast v-SNARE Vti1p mediates two vesicle transport pathways through interactions with the t-SNAREs Sed5p and Pep12p. *J. Cell Biol.* 137:1511–1524.

Walter, D.M., K.S. Paul, and M.G. Waters. 1998. Purification and characterization of a novel 13 S hetero-oligomeric protein complex that stimulates in vitro Golgi transport. *J. Biol. Chem.* 273:29565–29576.

Wang, W., M. Sacher, and S. Ferro-Novick. 2000. TRAPP stimulates guanine nucleotide exchange on Ypt1p. *J. Cell Biol.* 151:289–296.

Waters, M.G., D.O. Clary, and J.E. Rothman. 1992. A novel 115-kD peripheral membrane protein is required for intercisternal transport in the Golgi stack. *J. Cell Biol.* 118:1015–1026.

Whyte, J.R., and S. Munro. 2001. The Sec34/35 Golgi transport complex is related to the exocyst, defining a family of complexes involved in multiple steps of membrane traffic. *Dev. Cell*. 1:527–537.

Whyte, J.R., and S. Munro. 2002. Vesicle tethering complexes in membrane traffic. *J. Cell Sci.* 115:2627–2637.

Williams, A.L., S. Ehm, N.C. Jacobson, D. Xu, and J.C. Hay. 2004. rsly1 binding to syntaxin 5 is required for endoplasmic reticulum-to-Golgi transport but does not promote SNARE motif accessibility. *Mol. Biol. Cell*. 15:162–175.

Wu, X., R.A. Steet, O. Bohorov, J. Bakker, J. Newell, M. Krieger, L. Spaapen, S. Kornfeld, and H.H. Freeze. 2004. Mutation of the COG complex subunit gene COG7 causes a lethal congenital disorder. *Nat. Med.* 10:518–523.

Wuestehube, L.J., R. Duden, A. Eun, S. Hamamoto, P. Korn, R. Ram, and R. Schekman. 1996. New mutants of *Saccharomyces cerevisiae* affected in the transport of proteins from the endoplasmic reticulum to the Golgi complex. *Genetics*. 142:393–406.

Wurmser, A.E., T.K. Sato, and S.D. Emr. 2000. New component of the vacuolar class C-Vps complex couples nucleotide exchange on the Ypt7 GTPase to SNARE-dependent docking and fusion. *J. Cell Biol.* 151:551–562.

Zolov, S.N., and V.V. Lupashin. 2005. Cog3p depletion blocks vesicle-mediated Golgi retrograde trafficking in HeLa cells. *J. Cell Biol.* 168:747–759.